

Ground state energy of unitary Fermi gas from the ϵ expansion

Yusuke Nishida

Institute for Nuclear Theory, University of Washington, Seattle, Washington 98195-1550, USA

(Dated: March 21, 2019)

We update the ground state energy ratio of unitary Fermi gas to noninteracting Fermi gas (ξ) from the ϵ expansion by including the next-to-next-to-leading-order (NNLO) term near two spatial dimensions. Interpolations of the NNLO ϵ expansions around four and two spatial dimensions with the use of Padé approximants give $\xi \approx 0.403 \pm 0.031$ in three dimensions. This value is consistent with the previous interpolations of the NLO ϵ expansions $\xi \approx 0.377 \pm 0.013$ in spite of the large NNLO corrections.

PACS numbers: 03.75.Ss, 05.30.Fk

I. INTRODUCTION

Two-component fermions interacting via a zero-range and infinite scattering length interaction have attracted intense attention across many subfields of physics [1]. Experimentally, such a system can be realized in trapped atoms using the Feshbach resonance and has been extensively studied [2]. The most important property of the system is the scale invariance of the interaction, and thus, it can be thought of a rare realization of nonrelativistic conformal field theories [3–6].

As a consequence of the scale invariance of the interaction, all physical quantities at finite density and zero temperature are determined by simple dimensional analysis up to dimensionless constants of proportionality. Such dimensionless parameters are universal depending only on the dimensionality of space. A representative example of the universal parameters is the ground state energy of the Fermi gas at infinite scattering length (unitary Fermi gas) normalized by that of a noninteracting Fermi gas with the same density:

$$\xi_d \equiv \frac{E_{\text{unitary}}}{E_{\text{free}}}. \quad (1)$$

Here we put a subscript d to emphasize that ξ_d is a function of the dimensionality of space. Because ξ_d is a fundamental quantity characterizing the unitary Fermi gas, there have been substantial efforts to determine its value in $d = 3$ both from experiments [7–13] and Monte Carlo simulations [14–23].

For analytical treatments, the scale invariant interaction implies great difficulties because there seems to be no parameter to control a theory. However, it was shown that the problem of unitary Fermi gas can be solved systematically with appropriately formulated perturbation theories if the dimensionality of space d is close to four or close to two [24–26]. This is inspired by the special nature of four and two spatial dimensions for the zero-range and infinite scattering length interaction [27]: the unitary Fermi gas becomes a noninteracting Bose gas in $d = 4$ ($\xi_{d \rightarrow 4} \rightarrow 0$) while it becomes a noninteracting Fermi gas in $d = 2$ ($\xi_{d \rightarrow 2} \rightarrow 1$). Corrections to ξ_d near four and two spatial dimensions have been computed up to next-to-next-to-leading orders (NNLO) in terms of $\epsilon = 4 - d$

and $\bar{\epsilon} = d - 2$ [24, 25, 28, 29]:

$$\xi_{4-\epsilon} = \frac{\epsilon^{(6-\epsilon)/(4-\epsilon)}}{2} \times [1 - 0.04916 \epsilon - 0.95961 \epsilon^2 + O(\epsilon^3)] \quad (2)$$

and

$$\xi_{2+\bar{\epsilon}} = 1 - \bar{\epsilon} + 1.80685 \bar{\epsilon}^2 + O(\bar{\epsilon}^3). \quad (3)$$

Because NNLO corrections turn out to be large, naive extrapolations of the ϵ and $\bar{\epsilon}$ expansions to the physical case in $d = 3$ do not work at all. The more appropriate way to obtain the value of ξ_d in $d = 3$ is to interpolate the two expansions. This procedure has been carried out by using the next-to-leading-order (NLO) expansions around $d = 4$ and $d = 2$ [25] and by using the NNLO expansion around $d = 4$ and the NLO expansion around $d = 2$ [28] and reasonable agreement with results from Monte Carlo simulations was found.

The purpose of this paper is to update ξ_d in $d = 3$ by including the NNLO term near two spatial dimensions. First, we review the interpolations of the NLO ϵ expansions to see the stability of the results to the choice of interpolation schemes (Sec. II). We then show results from the interpolations of the NNLO ϵ expansions in Sec. III. Finally, summary and concluding remarks are given in Sec. IV. The NNLO correction to ξ_d near $d = 2$ shown in Eq. (3) is computed in the Appendix.

II. INTERPOLATIONS OF NLO EXPANSIONS

In order to see the stability of the results to the choice of interpolation schemes, we review the interpolations of the NLO ϵ expansions by using Padé approximants with and without applying the Borel transformation.

A. Padé interpolation

The simplest way to interpolate the two expansions around $d = 4$ and $d = 2$ is to use the Padé approximants.

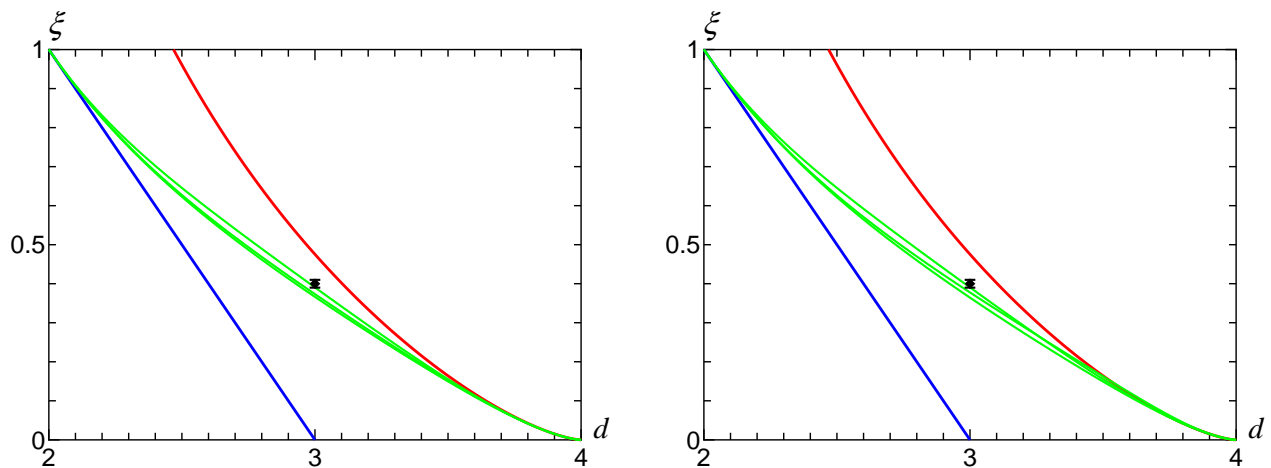


FIG. 1: The universal parameter ξ_d as a function of spatial dimensions d . The upper curve is the extrapolation from the NLO expansion around $d = 4$ in Eq. (2), while the lower line is the extrapolation from the NLO expansion around $d = 2$ in Eq. (3). The middle three curves show the Padé (left panel) or Borel-Padé [25] (right panel) interpolations of the two NLO expansions. The symbol at $d = 3$ indicates the result $\xi_3 \approx 0.40(1)$ from the latest Monte Carlo simulations [21, 23].

We write ξ_d in Eq. (2) in the following form:

$$\xi_{4-\epsilon} = \frac{\epsilon^{(6-\epsilon)/(4-\epsilon)}}{2} F(\epsilon), \quad (4)$$

where $F(\epsilon)$ is an unknown function having the expansion $F(\epsilon) = 1 - 0.04916\epsilon - 0.95961\epsilon^2 + O(\epsilon^3)$ [35]. We approximate $F(\epsilon)$ by a ratio of two polynomials (Padé approximant),

$$F_{[M/N]}(\epsilon) = \frac{p_0 + p_1\epsilon + \dots + p_M\epsilon^M}{1 + q_1\epsilon + \dots + q_N\epsilon^N}, \quad (5)$$

and determine the unknown coefficients so that ξ_d has the correct expansions around $d = 4$ and $d = 2$. If one truncates the ϵ and $\bar{\epsilon}$ expansions at NLO, we have four known terms and thus Padé approximants $F_{[M/N]}$ satisfying $M + N = 3$ are possible. We exclude the possibility of $F_{[1/2]}(\epsilon)$ because it has a pole in a range $0 < \epsilon < 2$ while we expect a smooth behavior of ξ_d as a function of $2 < d < 4$.

The left panel in Fig. 1 shows the universal parameter ξ_d as a function of d . The middle three curves show the Padé interpolations of the two NLO expansions with the use of $F_{[3/0]}$, $F_{[1/2]}$, and $F_{[0/3]}$. In $d = 3$, these interpolations, respectively, give

$$\xi_3 \approx 0.391, \quad 0.366, \quad 0.373. \quad (6)$$

These values span a small interval $\xi_3 \approx 0.378 \pm 0.012$. We note that the same interpolation scheme was employed to compute the lowest two energy levels of three fermions in a harmonic potential and excellent agreement with the exact results was found in arbitrary spatial dimensions $2 < d < 4$ [5].

B. Borel-Padé interpolation

The other way to interpolate the two expansions is to apply the Borel transformation and then use the Padé approximants [25]. We first rewrite the unknown function $F(\epsilon)$ in Eq. (4) in the form of the Borel transformation:

$$F(\epsilon) = \frac{1}{\epsilon} \int_0^\infty dt e^{-t/\epsilon} G(t). \quad (7)$$

If $F(\epsilon)$ has an expansion $F(\epsilon) = \sum_{n=0}^\infty c_n \epsilon^n$, $G(t)$ has an expansion $G(t) = \sum_{n=0}^\infty \frac{c_n}{n!} t^n$, and thus, the Borel transformation makes the expansion faster convergent. Then we approximate $G(t)$ by the Padé approximant,

$$G_{[M/N]}(t) = \frac{p_0 + p_1 t + \dots + p_M t^M}{1 + q_1 t + \dots + q_N t^N}, \quad (8)$$

and determine the unknown coefficients so that ξ_d has the correct expansions around $d = 4$ and $d = 2$.

The right panel in Fig. 1 shows the universal parameter ξ_d as a function of d . The middle three curves show the Borel-Padé interpolations of the two NLO expansions with the use of $G_{[3/0]}$, $G_{[1/2]}$, and $G_{[0/3]}$. The possibility of $G_{[2/1]}$ is excluded because we could not find a solution satisfying the constraints of Eqs. (2) and (3). In $d = 3$, these interpolations, respectively, give [25]

$$\xi_3 \approx 0.391, \quad 0.364, \quad 0.378. \quad (9)$$

These values span a small interval $\xi_3 \approx 0.377 \pm 0.013$. We note that the result of $G_{[3/0]}$ is equivalent to that of $F_{[3/0]}$ in Eq. (6).

Comparing the results in Eqs. (6) and (9), one can see that the interpolated values do not depend much on the choice of the Padé approximants and also the Borel transformation does not improve the interpolated values.

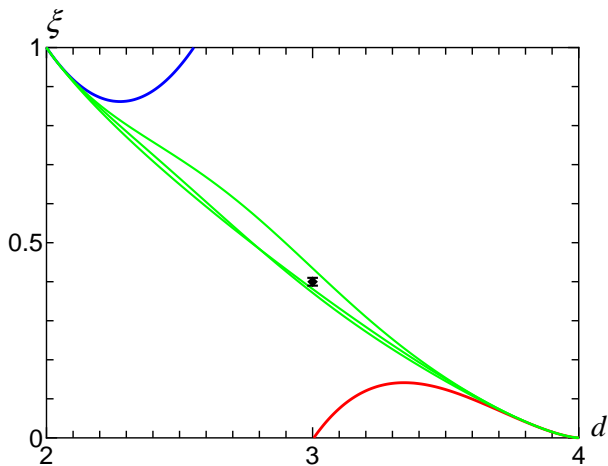


FIG. 2: The universal parameter ξ_d as a function of spatial dimensions d . The lower right curve is the extrapolation from the NNLO expansion around $d = 4$ in Eq. (2), while the upper left curve is the extrapolation from the NNLO expansion around $d = 2$ in Eq. (3). The middle three curves show the Padé interpolations of the two NNLO expansions. The symbol at $d = 3$ indicates the result $\xi_3 \approx 0.40(1)$ from the latest Monte Carlo simulations [21, 23].

The latter can be understood because we have only a few terms in the expansion over ϵ (two terms up to NLO), the advantage to apply the Borel transformation is little. This situation does not change even if we include the NNLO term near $d = 4$. The use of the Borel transformation may become essential once we have more higher-order corrections.

III. PADÉ INTERPOLATION OF NNLO EXPANSIONS

We now include the NNLO terms near $d = 4$ and $d = 2$ to interpolate the two expansions. Here we only use the Padé interpolation by the above-mentioned reason. Because we have six known terms, Padé approximants $F_{[M/N]}$ satisfying $M + N = 5$ are possible. However, we exclude the possibility of $F_{[4/1]}$, $F_{[2/3]}$, and $F_{[1/4]}$ because they have poles in a range $0 < \epsilon < 2$ while we expect a smooth behavior of ξ_d as a function of $2 < d < 4$.

Fig. 2 shows the universal parameter ξ_d as a function of d . The middle three curves show the Padé interpolations of the two NNLO expansions with the use of $F_{[5/0]}$, $F_{[3/2]}$, and $F_{[0/5]}$. In $d = 3$, these interpolations, respectively, give

$$\xi_3 \approx 0.372, \quad 0.381, \quad 0.435. \quad (10)$$

These values span a larger interval $\xi_3 \approx 0.403 \pm 0.031$. It is understandable that the interpolations of the NNLO expansions have a larger uncertainty because of the large NNLO corrections both near $d = 4$ and $d = 2$ [see Eqs. (2) and (3) and also Fig. 2]. What is remarkable is that in

spite of such large NNLO corrections, the interpolated values are consistent with the previous interpolations of the NLO expansions $\xi_3 \approx 0.377 \pm 0.013$. Therefore we conclude that the interpolated results are stable to inclusion of higher-order corrections and thus the ϵ expansion has a certain predictive power even though the knowledge on higher-order terms in the expansions over $\epsilon = 4 - d$ and $\bar{\epsilon} = d - 2$ is currently lacking.

IV. SUMMARY AND CONCLUDING REMARKS

In this paper, we have updated the ground state energy ratio of unitary Fermi gas to noninteracting Fermi gas (ξ) from the ϵ expansion by including the NNLO term near two spatial dimensions. We found that the Padé interpolations of the NNLO expansions around $d = 4$ and $d = 2$ give $\xi \approx 0.403 \pm 0.031$ in $d = 3$. Although the NNLO corrections are large both near $d = 4$ and $d = 2$, the interpolated value is consistent with the interpolations of the NLO expansions $\xi \approx 0.377 \pm 0.013$. This indicates that the interpolated results are stable to inclusion of higher-order corrections and thus the ϵ expansion has a certain predictive power. Indeed, our interpolated values reasonably agree with the results from the latest Monte Carlo simulations, $\xi \approx 0.40$ [21] and $\xi \lesssim 0.40(1)$ [23].

Our analysis also implies that in order to obtain appropriate results from the ϵ expansion, it is necessary to incorporate the expansions both around $d = 4$ and $d = 2$. Other than ξ studied in this paper, interpolations of NLO expansions around $d = 4$ and $d = 2$ have been employed to estimate the critical temperature T_c [26], thermodynamic functions at T_c [26], and the ground state energy of a few fermions in a harmonic potential [5]. Quasi-particle spectrum [24, 25], atom-dimer and dimer-dimer scatterings in vacuum [30], phase structure of polarized Fermi gas [25, 31], BCS-BEC crossover [32], momentum distribution and condensate fraction [29], low-energy dynamics [33], and energy density functional [34] have been studied only in the expansions over $\epsilon = 4 - d$. It is possible to obtain better understanding on these subjects by further incorporating the expansions in terms of $\bar{\epsilon} = d - 2$.

Acknowledgments

The author thanks D. Gazit for discussions. This work was supported, in part, by JSPS Postdoctoral Program for Research Abroad.

APPENDIX: NNLO CORRECTION TO ξ_d NEAR $d = 2$

In this Appendix, we briefly review the $\bar{\epsilon}$ expansion for the unitary Fermi gas around two spatial dimensions and compute the NNLO correction to ξ_d in terms of $\bar{\epsilon} = d - 2$

shown in Eq. (3). The detailed account of the $\bar{\epsilon}$ expansion is found in Ref. [25].

1. Lagrangian and power counting rule of $\bar{\epsilon}$

The unitary Fermi gas near two spatial dimensions is described by the sum of following Lagrangian densities (here and below $\hbar = 1$):

$$\mathcal{L}_0 = \sum_{\sigma=\uparrow,\downarrow} \psi_\sigma^\dagger \left(i\partial_t + \frac{\nabla^2}{2m} + \mu \right) \psi_\sigma \quad (\text{A.1})$$

$$\mathcal{L}_1 = -\varphi^* \varphi + \bar{g} \varphi^* \psi_\downarrow \psi_\uparrow + \bar{g} \psi_\downarrow^\dagger \psi_\uparrow^\dagger \varphi \quad (\text{A.2})$$

$$\mathcal{L}_2 = \varphi^* \varphi. \quad (\text{A.3})$$

Here we have neglected the condensate $\phi_0 \sim \mu e^{-1/\bar{\epsilon}}$, because its contribution is negligible compared to any power corrections of $\bar{\epsilon}$.

The first part \mathcal{L}_0 generates the propagator of fermionic field ψ_σ ,

$$G(p_0, \mathbf{p}) = \frac{1}{p_0 - \varepsilon_{\mathbf{p}} + \mu + i\delta}, \quad (\text{A.4})$$

where $\varepsilon_{\mathbf{p}} = \mathbf{p}^2/(2m)$ is the kinetic energy of nonrelativistic particles. The second part \mathcal{L}_1 describes the interaction between fermions mediated by the auxiliary field φ . The first term in \mathcal{L}_1 gives the propagator of φ ,

$$D(p_0, \mathbf{p}) = -1, \quad (\text{A.5})$$

and the last two terms give vertices coupling two fermions with φ . The coupling constant \bar{g} is given by

$$\bar{g} = \left(\frac{2\pi\bar{\epsilon}}{m} \right)^{1/2} \left(\frac{m\mu}{2\pi} \right)^{-\bar{\epsilon}/4}. \quad (\text{A.6})$$

Here the factor $(m\mu/2\pi)^{-\bar{\epsilon}/4}$ was introduced so that the product of auxiliary fields $\varphi^* \varphi$ has the same dimension as the Lagrangian density. We stress that the choice of this factor is arbitrary, if it has the correct dimension, and does not affect final results because the difference can be absorbed by the redefinition of φ . The particular choice of \bar{g} in Eq. (A.6) will simplify expressions for loop integrals in intermediate steps.

If we did not have the last part \mathcal{L}_2 , we could integrate out the auxiliary fields φ and φ^* to lead to

$$\mathcal{L}_1 \rightarrow \bar{g}^2 \psi_\uparrow^\dagger \psi_\downarrow^\dagger \psi_\downarrow \psi_\uparrow, \quad (\text{A.7})$$

which represents the contact interaction of fermions with the small coupling $\bar{g}^2 \sim \bar{\epsilon}$. Therefore, the unitary Fermi gas near two spatial dimensions is simply described by a weakly-interacting system of fermions. The vertex in \mathcal{L}_2 plays a role of a counterterm so as to avoid double counting of a certain type of diagrams which is already taken into \mathcal{L}_1 .

The power counting rule of $\bar{\epsilon}$ is summarized as follows.



FIG. 3: Power counting rule of $\bar{\epsilon}$. The self-energy diagram of φ field (a) is combined with the vertex from \mathcal{L}_2 (b) to achieve the simple $\bar{\epsilon}$ counting. Solid (dotted) lines represent the fermion (auxiliary field) propagators iG (iD).

1. For any Green's function, we write down all Feynman diagrams using the propagator from \mathcal{L}_0 and the vertices from \mathcal{L}_1 .
2. If there is any subdiagram of the type in Fig. 3(a), we add the same Feynman diagram where the subdiagram is replaced by the vertex from \mathcal{L}_2 in Fig. 3(b).
3. The power of $\bar{\epsilon}$ for the given Feynman diagram is simply $O(\bar{\epsilon}^{N_{\bar{g}}/2})$, where $N_{\bar{g}}$ is the number of couplings \bar{g} .

Here the dimensional regularization of loop integrals is assumed.

2. Computation of the pressure

The pressure of unitary Fermi gas has been computed up to the next-to-leading order in $\bar{\epsilon}$ [25]. To the leading order, the pressure is given by that of noninteracting fermions:

$$\begin{aligned} P_{\text{free}} &= 2 \int \frac{d\mathbf{p}}{(2\pi)^d} (\mu - \varepsilon_{\mathbf{p}}) \theta(\mu - \varepsilon_{\mathbf{p}}) \\ &= \frac{2\mu}{\Gamma(\frac{d}{2} + 2)} \left(\frac{m\mu}{2\pi} \right)^{d/2}. \end{aligned} \quad (\text{A.8})$$

The $O(\bar{\epsilon})$ correction is given by the two-loop diagram depicted in Fig. 4, which represents the mean-field correction:

$$\begin{aligned} P_2 &= \bar{g}^2 \left[\int \frac{d\mathbf{p}}{(2\pi)^d} \theta(\mu - \varepsilon_{\mathbf{p}}) \right]^2 \\ &= \frac{\bar{\epsilon} \mu}{\Gamma(\frac{d}{2} + 1)^2} \left(\frac{m\mu}{2\pi} \right)^{\frac{d}{2}}. \end{aligned} \quad (\text{A.9})$$

To the next-to-next-to-leading order in $\bar{\epsilon}$, the pressure receives an $O(\bar{\epsilon}^2)$ correction from the three-loop diagram depicted in Fig. 4, which is evaluated as [29]

$$\begin{aligned} P_3 &= \bar{g}^2 \int \frac{d\mathbf{k} d\mathbf{p}}{(2\pi)^{2d}} \theta(\mu - \varepsilon_{\mathbf{p}+\frac{\mathbf{k}}{2}}) \theta(\mu - \varepsilon_{\mathbf{p}-\frac{\mathbf{k}}{2}}) \\ &\quad \times \left[1 + \bar{g}^2 \int \frac{d\mathbf{q}}{(2\pi)^d} \frac{\theta(\varepsilon_{\mathbf{q}+\frac{\mathbf{k}}{2}} - \mu) \theta(\varepsilon_{\mathbf{q}-\frac{\mathbf{k}}{2}} - \mu)}{2\varepsilon_{\mathbf{q}} - 2\varepsilon_{\mathbf{p}}} \right]. \end{aligned} \quad (\text{A.10})$$

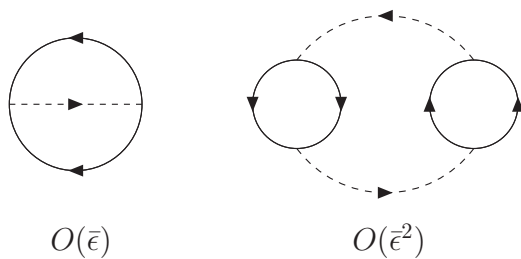


FIG. 4: Vacuum diagrams contributing to the pressure up to the next-to-next-to-leading order in $\bar{\epsilon}$. The counter vertex in Fig. 3(b) for each bubble diagram is implicitly understood for the $O(\bar{\epsilon}^2)$ diagram.

Here the frequency integrations are already performed. Note that $+1$ in the square brackets comes from the counter vertex in \mathcal{L}_2 . Due to the θ -functions, the ranges of integrations over $\varepsilon_{\mathbf{k}}$, $\varepsilon_{\mathbf{p}}$, and $\varepsilon_{\mathbf{q}}$ are limited to $0 \leq \varepsilon_{\mathbf{k}} \leq 4\mu$, $0 \leq \varepsilon_{\mathbf{p}} \leq \Lambda_p$, and $\Lambda_q \leq \varepsilon_{\mathbf{q}}$, where

$$\sqrt{\Lambda_p} = \frac{-|\cos \chi_p| \sqrt{\varepsilon_{\mathbf{k}}} + \sqrt{4\mu - \varepsilon_{\mathbf{k}} \sin^2 \chi_p}}{2} \quad (\text{A.11})$$

and

$$\sqrt{\Lambda_q} = \frac{|\cos \chi_q| \sqrt{\varepsilon_{\mathbf{k}}} + \sqrt{4\mu - \varepsilon_{\mathbf{k}} \sin^2 \chi_q}}{2} \quad (\text{A.12})$$

with $\cos \chi_p = \hat{\mathbf{k}} \cdot \hat{\mathbf{p}}$ and $\cos \chi_q = \hat{\mathbf{k}} \cdot \hat{\mathbf{q}}$. The integration over $\varepsilon_{\mathbf{q}}$ can be performed analytically using the dimensional regularization. As a result, the expression in the square brackets in Eq. (A.10) becomes

$$[\dots] = -\frac{\gamma}{2} \bar{\epsilon} - \frac{\bar{\epsilon}}{2} \int_0^\pi \frac{d\chi_q}{\pi} \ln \left(\frac{\Lambda_q - \varepsilon_{\mathbf{p}}}{\mu} \right) + O(\bar{\epsilon}^2). \quad (\text{A.13})$$

Then, introducing dimensionless variables $z = \varepsilon_{\mathbf{k}}/\mu$, $\tilde{\Lambda}_{p(q)} = \Lambda_{p(q)}/\mu$ and performing the integration over

$\varepsilon_{\mathbf{p}}/\mu$, we obtain the following expression for P_3 :

$$P_3 = -\bar{\epsilon}^2 \frac{m\mu^2}{2\pi} \left[\frac{\gamma}{2} + \frac{1}{2} \int_0^4 dz \int_0^\pi \frac{d\chi_p}{\pi} \int_0^\pi \frac{d\chi_q}{\pi} \times \left\{ \tilde{\Lambda}_q \ln \tilde{\Lambda}_q - (\tilde{\Lambda}_q - \tilde{\Lambda}_p) \ln(\tilde{\Lambda}_q - \tilde{\Lambda}_p) - \tilde{\Lambda}_p \right\} \right]. \quad (\text{A.14})$$

Finally the numerical integrations over z , χ_p , and χ_q lead to

$$P_3 = -\bar{\epsilon}^2 \frac{m\mu^2}{2\pi} \left(\frac{\gamma}{2} + 0.0568528 \right) + O(\bar{\epsilon}^3). \quad (\text{A.15})$$

Consequently, we obtain the pressure up to the next-to-next-to-leading order in $\bar{\epsilon}$ as

$$P = P_{\text{free}} + P_2 + P_3 = P_{\text{free}} \left[1 + \bar{\epsilon} - 0.3068528 \bar{\epsilon}^2 + O(\bar{\epsilon}^3) \right]. \quad (\text{A.16})$$

The universal parameter of the unitary Fermi gas in Eq. (1) can be equivalently expressed as $\xi_d = \mu/\varepsilon_F$. From the thermodynamic relationship $n = \partial P/\partial \mu$ and the definition of the Fermi energy in d spatial dimensions,

$$\varepsilon_F = \frac{2\pi}{m} \left[\frac{1}{2} \Gamma \left(\frac{d}{2} + 1 \right) n \right]^{2/d}, \quad (\text{A.17})$$

we can determine ξ_d from the $\bar{\epsilon}$ expansion to be

$$\xi_{2+\bar{\epsilon}} = \left[1 + \bar{\epsilon} - 0.3068528 \bar{\epsilon}^2 \right]^{-\frac{2}{2+\bar{\epsilon}}} = 1 - \bar{\epsilon} + 1.8068528 \bar{\epsilon}^2 + O(\bar{\epsilon}^3). \quad (\text{A.18})$$

This is the result shown in Eq. (3). Although the $O(\bar{\epsilon}^2)$ correction to the pressure is relatively small, the NNLO correction to $\xi_{2+\bar{\epsilon}}$ turns out to be sizable because of the large $O(\bar{\epsilon})$ correction in the pressure.

-
- [1] For recent reviews, see I. Bloch, J. Dalibard, and W. Zwerger, *Rev. Mod. Phys.* **80**, 885 (2008); S. Giorgini, L. P. Pitaevskii, and S. Stringari, arXiv:0706.3360 [cond-mat.other].
- [2] W. Ketterle and M. W. Zwierlein, arXiv:0801.2500 [cond-mat.other], and references therein.
- [3] T. Mehen, I. W. Stewart, and M. B. Wise, *Phys. Lett. B* **474**, 145 (2000).
- [4] D. T. Son and M. Wingate, *Annals Phys.* **321**, 197 (2006).
- [5] Y. Nishida and D. T. Son, *Phys. Rev. D* **76**, 086004 (2007).
- [6] T. Mehen, arXiv:0712.0867 [cond-mat.other].
- [7] K. M. O'Hara *et al.*, *Science* **298**, 2179 (2002).
- [8] M. Bartenstein *et al.*, *Phys. Rev. Lett.* **92**, 120401 (2004).
- [9] T. Bourdel *et al.*, *Phys. Rev. Lett.* **93**, 050401 (2004).
- [10] J. Kinast *et al.*, *Science* **307**, 1296 (2005).
- [11] G. B. Partridge *et al.*, *Science* **311**, 503 (2006).
- [12] J. T. Stewart *et al.*, *Phys. Rev. Lett.* **97**, 220406 (2006).
- [13] L. Tarruell *et al.*, arXiv:cond-mat/0701181.
- [14] J. Carlson, S.-Y. Chang, V. R. Pandharipande, and K. E. Schmidt, *Phys. Rev. Lett.* **91**, 050401 (2003).
- [15] S. Y. Chang, V. R. Pandharipande, J. Carlson, and K. E. Schmidt, *Phys. Rev. A* **70**, 043602 (2004).
- [16] G. E. Astrakharchik, J. Boronat, J. Casulleras, and S. Giorgini, *Phys. Rev. Lett.* **93**, 200404 (2004).
- [17] J. Carlson and S. Reddy, *Phys. Rev. Lett.* **95**, 060401 (2005).
- [18] A. Bulgac, J. E. Drut, and P. Magierski, *Phys. Rev. Lett.* **96**, 090404 (2006).
- [19] D. Lee, *Phys. Rev. B* **73**, 115112 (2006).
- [20] T. Abe and R. Seki, arXiv:0708.2524 [nucl-th].

- [21] A. Bulgac, J. E. Drut, P. Magierski, and G. Wlazlowski, arXiv:0801.1504 [cond-mat.stat-mech].
- [22] D. Lee, Phys. Rev. C **78**, 024001 (2008).
- [23] S. Zhang, K. E. Schmidt, and J. Carlson, unpublished.
- [24] Y. Nishida and D. T. Son, Phys. Rev. Lett. **97**, 050403 (2006).
- [25] Y. Nishida and D. T. Son, Phys. Rev. A **75**, 063617 (2007).
- [26] Y. Nishida, Phys. Rev. A **75**, 063618 (2007).
- [27] Z. Nussinov and S. Nussinov, Phys. Rev. A **74**, 053622 (2006).
- [28] P. Arnold, J. E. Drut, and D. T. Son, Phys. Rev. A **75**, 043605 (2007).
- [29] Y. Nishida, Ph.D. Thesis, University of Tokyo, 2007 [available as arXiv:cond-mat/0703465v2].
- [30] G. Rupak, arXiv:nucl-th/0605074.
- [31] G. Rupak, T. Schafer, and A. Kryjevski, Phys. Rev. A **75**, 023606 (2007).
- [32] J. W. Chen and E. Nakano, Phys. Rev. A **75**, 043620 (2007).
- [33] A. Kryjevski, arXiv:0712.2093 [nucl-th]; arXiv:0804.2919 [nucl-th].
- [34] G. Rupak and T. Schafer, arXiv:0804.2678 [nucl-th].
- [35] It has been shown that there is a nonanalytic term $-\frac{3}{8}\epsilon^3 \ln \epsilon$ to the next-to-next-to-next-to-leading order in ϵ [28]. Because we are working up to NNLO in the current paper, we neglect such a nonanalytic contribution.